Response to Reviewer #1:

We thank the reviewer for carefully reading our manuscript and for providing highly valuable comments, which we have addressed in detail below.

Major comments:

In the abstract, lines 18-20, the EVR configuration is presented primarily as an improvement by passivating surfaces, with "further improvement" by heating to 120 C. However, as far as I can tell, there is no data presented in the manuscript about how much the passivated surfaces changed the response times. If the authors want to highlight the passivation, this type of information needs to be included in some form. Otherwise, the temperature increase, for which there is clear data (e.g. Fig. 3a), should be presented as the main improvement. And in that case, the novelty of this manuscript (and the EVR inlet) is questionable, as there are a wealth of PTR studies where inlets and inlet lines have been heated in order to improve response times and detection of less volatile species (see e.g. section 2.4.5 in Yuan et al., 2017, Chem. Rev.). The authors need to make very clear what exactly causes the improvement of response times in this manuscript, and how this is different enough from earlier work that it deserves publication in AMT.

We have found data from two experiments wherein the signal decay of *cis*-pinonic acid was measured with the same instrument, before and after being modified to the EVR configuration. All other experimental parameters were kept identical. The signal decay time dropped from $\tau_{1/e}$ = 181 s to $\tau_{1/e}$ = 4 s. In the revised manuscript, we are presenting these data as the first results in the Results section, clearly demonstrating and highlighting the benefit of surface passivation.

Lines 55-58 at the end of the introduction do not even mention the temperature issue, suggesting that the material changes are the main topic of this manuscript. This requires verification.

We refer to our comment above, but agree that the effect of temperature should be mentioned in the Introduction. The revised paragraph reads as follows:" Herein we will demonstrate how the use of heated inlet capillaries made of passivated stainless steel (SS) and of a heated drift tube with passivated metal surfaces significantly improves the time response performance of PTR-MS analyzers. We will show that the heated and passivated instrument responds fast to low-volatility analytes, both for gas-phase and particle-phase measurements."

A related point is the lack of any schematic diagram of the EVR in the manuscript. It may be understandable if the design itself did not change, but rather only materials were exchanged, yet it would still be beneficial for a reader to see a figure showing these changes. As it is, the only reference on PTR in section 2.1 is the Yuan et al (2017) review, which itself doesn't have a schematic of the exact system used in this work. This makes it very laborious for a reader to understand the changes, and consequently to properly assess the novelty of the changes and the manuscript itself.

This is a valuable suggestion and we have included a figure (new Fig. 1) showing the drift tube and inlet system with all passivated surfaces in the Experimental section.

Specific comments:

1. Lines 28-29: Since these measurements were done using NH4+ adducts, I don't think it should any longer be called "PTR-MS".

PTR-MS instruments can nowadays be operated with different chemical ionization reagent ions (H_3O^+, NO^+, O_2^+, NH_4^+, others), and most of them do not react via proton transfer reactions (PTR). It is debatable if it makes sense to introduce additional acronyms for different operation modes of the same instrument. In the past, the acronym "eTR-MS" has been proposed for the O_2^+ mode but it was never taken up by the community. Our operation mode should probably be called "AAF-MS" (AAF: Ammonium Adduct Formation). We think that introducing new acronyms for different operation modes of the same instrument would just create confusion. Note that we are referring to the PTR-MS instrument and not to PTR-MS as a chemical ionization method.

2. Lines 69-70. Since T_drift is used later as a parameter, it is important for a reader to have a clear picture of how the drift tube looks. Also here a schematic would be useful.

As stated above, we have included a figure showing the drift tube and inlet system in the Experimental section.

3. Lines 50-51: "H3O+ ion chemistry thus detects a wider spectrum of analytes than any other chemical ionization method for atmospheric organic carbon." This is a strong statement and would need a citation. Instruments like the NH4+-CI3-TOF or C3H7NH3+-APi-TOF (Berndt et al., 2018, Angew. Chem. Int. Ed. 2018, 57, 3820 –3824) seem to detect almost all organic compounds (including radicals) except hydrocarbons. Can the authors show references where H3O+ ion chemistry would have detected a broader spectrum than that?

Well, basic ion chemistry tells us that H_3O^+ ions react with a broader spectrum of organic species than NH_4^+ or $C_3H_7NH_3^+$ ions. The scope of this paper is, however, not to discuss the pros and cons of different reagent ions. Since Reviewer 2 also did not like our comparative statement, we have removed it.

4. Lines 73-75. These two sentences need to be reformulated. "was measured as the time that evolved until" is hard to understand.

We changed our wording to: "$\tau_{1/e}$ is the time it took the analyte signal to decay to 1/e (36.8%) of its initial value. τ_{90} is the time it took the analyte signal to decay to 10% of its initial value."

5. Fig. S1. The part inside the red dashed box is presumably the inlet and drift tube of the PTR? This needs to be clarified, as it is not easy to read for someone not highly experienced with the system.

Fig. S1 has been revised to better show the experimental set-up. Additional details are shown in the newly included Fig.1.

6. Lines 108-109: This leaves the reader with the question "why?".

It was more difficult to generate low volume mixing rations with these substances. This is now explained in the text.

7. Lines 133-134: This also leaves the reader with the question "why?".

The solid *cis*-pinonic acid sample was heated to 70 °C for generating a measurable concentration in the gas phase. Using lower instrument temperatures would have resulted in condensation on the walls. This is now explained in the text.

8. Section 3.2: The discussion is about T_drift, and the text suggests that it is only the drift tube temperature that is changed. But Fig. S1 suggests that the entire inlet is one temperature-controlled entity. Please clarify. This again would be easier to understand if there was a proper schematic included.

Fig. 1, which has been newly included in the Experimental section, should make it clear what parts are heated in the temperature-controlled instrument enclosure.

9. Lines 138-139: This seems consistent, but Fig. S2 shows that the dependence of tau on C0 is very weak, with compounds of the same C0 easily having an order of magnitude or larger differences in tau. Were these two compounds selected to be shown because they happened to match?

Both our data and literature data indicate that for long-chain ketones and carboxylic acids $\tau_{1/e}$ exhibits the expected increase with decreasing log C^0, while for saccharides and substituted phenols other factors seem to play a role. We thus show data for one long-chain ketone and one carboxylic acid. This is explained in the text:" For long-chain ketones (Pagonis et al., 2017; Krechmer et al., 2018) and carboxylic acids (Fig. S2), $\tau_{1/e}$ exhibits the expected increase with decreasing log C^0. Since log C^0 depends upon temperature, changes in T_{drift} should lead to predictable changes in $\tau_{1/e}$. We thus measured $\tau_{1/e}$ for 2-tridecanone$_{(g)}$ and *cis*-pinonic acid$_{(g)}$ at variable T_{drift} (Fig. 5)."

10. Line 144: Why are you now shifting from tau_1/e to tau_90?

Some of the literature data were only reported as τ_{90}.

11. Line 145: It is unclear which data from this study is used in Fig. 4. This should be made clear, so that a reader would be able to compare responses compound by compound. In addition, there is a nice monotonic trend of tau vs C0 in Fig. 4, which is hard to understand given the huge spread of points in Fig. S2. One is left wondering how the authors selected the 5 data points shown in Fig. 4 for the EVR.

The compound names have been included on the upper x-axis of the figure. Comparing the time response of different instruments to different compounds is obviously difficult, and one needs to be careful not to compare apples with pears. Our data suggest that at least for carbonyls and carboxylic acids the observed trends in $\tau_{1/e}$ can be explained by differences in C_0, which is why we have only included such compounds in the figure. We explain this in the revised text:" The upper horizontal axis lists the compound names; the lower horizontal axis shows in which log C^0 range molecules are classified as volatile organic compounds (VOCs), intermediate volatility organic compounds (IVOCs) and semi-volatile organic compounds (SVOCs). Since the instruments did not measure the same SVOCs, we only use our carboxylic acid data for the log C^0-based comparison."

12. Line 153: C13 ketones are referenced, but I do not know where I should be looking to find this data.

The compound names have been included on the upper x-axis of the figure.

13. Fig. 4: It took me a while to realize that the unit of tau changes between Fig. 2 and Fig. 4, from sec to min. Why not keep them the same? Now both the time unit and the decay reference (1/e vs 90) change, and it makes things much harder to follow. I suggest to make all of these the same, as it would make the reading much smoother and avoid confusion.

All times are now reported in seconds.

14. Fig. 4: If I understand the plot correctly, the non-EVR PTR-TOF from this study seems to work much better than the EVR. All measured response times are on the order of 0.01min, while in the EVR all points

are at 0.1 min or higher. Does this mean that the EVR setup has actually made the response times worse compared to the original design (as long as the inlet is heated)?

Unfortunately, the reviewer has misinterpreted the figure. log C^0 is a measure of volatility and the compounds studied include volatile organic compounds (VOCs), intermediate-volatility organic compounds (IVOCs) and semi-volatile organic compounds (SVOCs). We have added a classification bar on the x-axis for including this information. As a general trend, τ_{90} increases with decreasing volatility or decreasing C_0. What the figure shows is the following:

i) For VOCs and the more volatile IVOCs (log $C^0 \geq 5$), τ_{90} is close to the volumetric exchange time of the drift tube for both the EVR and the conventional PTR-ToF-MS instrument, as long as the drift tube is heated to 120 °C. Conventional unheated PTR-MS instruments have a much slower time response.

ii) For the less volatile IVOCs (log $C^0 \leq 3$) and SVOCs, surface passivation reduces τ_{90} by two orders of magnitude (*cis*-pinonic acid), even if the drift tube is heated to 120 °C in both the conventional and the EVR PTR-ToF-Ms analyzer. The heated EVR PTR-ToF-MS responds as fast as state-of-the-art CIMS instruments.

We have adapted the text to convey the above information.

15. Line 155: The fact that temperature explains the major part of the differences, and this fact is only mentioned in one sentence in the main text, makes Fig. 4 very misleading. For example, one would read from Fig. 4 that the reason the PTR-TOF in this study was 3-4 orders of magnitude better than the PTR-qMS from Pagonis et al is related to the quad vs tof, since that is the only clear difference. Not to mention the comparison to other instruments, which were not run at elevated temperatures. Please put the operating temperatures into the figure legend, since these values are the most critical parameter to understand the major differences in the figure.

Temperature is certainly an important factor and we have included the operating temperatures in the figure legend. The key information is, however, that for the less volatile IVOCs (log $C^0 \leq 3$) and SVOCs an increase in the drift temperature to 120 °C alone does not do the job. It is the surface passivation that drops τ_{90} by two additional orders of magnitude.

16. Lines 171-172: Again, the fast changes are attributed to the materials, and temperature is not mentioned at all. This needs to be clearly validated before making this claim.

We have extensively addressed this issue in previous comments and in the revised manuscript.

17. Conflict of interest statement: Ionicon analytik is said to be "commercializing (CHARON) PTR-MS", but they are also advertising directly the EVR setup presented here (https://www.ionicon.com/accessories/details/extended-volatility-range-evr). Why is this not mentioned here?

We are now explicitly mentioning that IONICON Analytik commercializes PTR-MS, CHARON and EVR.

Technical corrections:

1. Line 97 and line 107: Caption, not legend.

This was corrected.

Response to Reviewer #2:

We thank the reviewer for carefully reading our manuscript and for providing highly valuable comments, which we have addressed in detail below.

Major comments:

1. The purpose and the focus of the manuscript are a little unclear. Is it just to estimate the signal-decay times for a new instrument or to assess its performance more holistically? If so, the effects of interactions with inlet walls and humidity should be discussed in this paper.

The main purpose of this manuscript is to establish the EVR PTR-MS instrument in the scientific literature. More than two dozens of EVR PTR-MS instruments are nowadays in use, and we think it is important that the users can refer to an instrument paper when presenting their own data. We want to present a new type of PTR-MS instrument and exemplify its improved performance, rather than systematically investigating material, temperature or humidity effects.

2. The effect of the drift tube temperature is interesting and important for more comprehensive evaluation of the instrument measurement capability, but is weakened by the very small number of compounds used to derive the conclusion that 120oC is the optimal temperature at which the instrument should be operated. It would be of interest to conduct similar measurements with a larger set of compounds, especially with the ones that tend to thermally decompose at higher temperatures, such as hydroperoxides (i.e., cumene hydroperoxide and dicumylperoxide discussed later in the paper).

While the suggested thermal decomposition study would certainly be interesting, we feel that such work would go beyond the scope of a first instrument paper (see reply to comment 1). Please also note that we are not claiming that 120 °C is the optimal operation temperature. In fact, the operation temperature must be adapted to the type of analytes that are to be measured. We are explicitly stating this in the revised manuscript.

3. I do not fully understand how detection of particle-phase highly oxidized organic compounds produced via ozonolysis of limonene fits in this paper. The authors neither discuss the signal-decay times for these compounds nor try to estimate the respective wall losses. It has been shown several times that softer ionization techniques, such as NH+ 4 CIMS, can be used for detection of highly oxygenated compounds in the gas and particle phase (i.e., Hansel et al., 2018; Zaytsev et al., 2019). Hence, the authors should clarify why they present these data and how implementation of the new inlet improves detection and quantification of these compounds.

We agree that we did not properly convey the information we wanted to give. Limonene ozonolysis was just a way for generating highly oxidized compounds up to O_8, which were not among the pure substances (up to O_6) available for our study. We have taken up the suggestion by the reviewer and show the signal decay of an O_8-compound. This demonstrates that even for highly oxidized analytes (ELVOC) $\tau_{1/e}$ remains below 20 s.

Specific comments:

1. Lines 49-54: From reading this paragraph one might get a false impression that PTR-MS has the best measurement capability among all CIMS instruments. While it is true that the ionization efficiency does not vary too much among oxidized and nonoxidized compounds, the overall measurement capability of

***PTR-MS instruments is significantly limited by ionic fragmentation and wall losses. Hence, the authors should edit this paragraph and make their description of PTR-MS more balanced*.**

We have only stated the H_3O^+ ion chemistry detects a broader spectrum of organic analytes than other CI techniques, which is certainly true from a pure ion chemistry point of view. This does *per se* not imply that PTR-MS has a better measurement capability, because the latter depends on additional factors (*e.g.*, inlet losses, detection limit). Since Reviewer 1 also did not like our comparative statement, we have removed it.

2. Lines 55-58: The effects of drift tube temperature are not mentioned here, however they seem to play a fairly important role as outlined in the Discussion section. The particle-phase experiments should also be mentioned at the end of Introduction.

This has also been pointed out by Reviewer 1 and we mention the effect of temperature in the revised paragraph. We also mention the particle experiments. The revised paragraph reads as follows:" Herein we will demonstrate how the use of heated inlet capillaries made of passivated stainless steel (SS) and of a heated drift tube with passivated metal surfaces significantly improves the time response performance of PTR-MS analyzers. We will show that the heated and passivated instrument responds fast to low-volatility analytes, both for gas-phase and particle-phase measurements."

3. Section 2.1: This section is missing a schematic of the EVR PTR-MS instrument. I suggest moving Fig S1 to the main text and significantly expanding it to demonstrate what parts of the instrument were replaced or coated. As of now, these changes might not be obvious especially for a reader who is not fully familiar with IONICON PTR-MS instruments.

The drift tube and capillary inlet system (including the passivated parts) are sketched in Figure 1 of the revised manuscript.

4. Line 95: Why did the authors use the double exponential decay for fitting the signals? How did the authors calculate τ1/e from fitted parameters b1 and b2? I believe this is not explicitly discussed in the paper.

We did not calculate $\tau_{1/e}$ from the fit. $\tau_{1/e}$ is simply the point in time when the analyte signal had dropped to 36% of its initial value. This is explicitly stated in the manuscript (§2.2). The fit was just included for guiding the eye; the fit function was included upon request of the editor.

5. Figure 2: What do different circles/data points for the same compound represent? The authors should clarify this and discuss why the difference between some data points is fairly large, for example for 2,6-dimethoxyphenol and diglycolic acid it can be up to a factor of 2.

See figure legend. Also see figure caption: „The size of the dots indicates the initial steady-state mixing ratio (0.1–100 ppbv) used in the respective experiment."

6. Lines 140-141: It would be beneficial if the authors could include high-resolution mass-spectra in the Supplement to demonstrate that studied compounds did not thermally decompose. Many of observed compounds are known to undergo ionic fragmentation (e.g., C6H9O + 4 is an ionic fragment of levoglucosan as discussed later in the paper), so how do the authors know that there is no additional thermal decomposition resulting in formation of those fragments?

The reviewer raises a good point; our statement was too general. What we can state is that we did not observe any decarboxylation products. This has been corrected in the revised manuscript:" Exposing the

sample gas to heated surfaces in an analyzer, may thermally degrade some analytes. It is important to note that none of the acids studied in this work decarboxylated at T_{drift} = 120°C. It may, however, be necessary to use a lower T_{drift} when more thermally labile analytes are targeted."

7. Section 3.3: The authors should provide a table in which they should list compounds that were used to compare performances of various instruments. What ketones, carboxylic acids and hydroxycarbonyls were used in this study?

The compound names have been included in the figure.

8. Figure 4: It seems to me that the authors did not measure response times for the same compounds using a conventional PTR-MS and a new EVR PTR-MS as yellow and dark red points are located far from each other (for yellow dots 5<logC0<7.3 while for dark red dots 0.5<logC0<5). I suggest that the authors include additional data points on this figure to demonstrate how the performance of the EVR PTR-MS instrument compares with a conventional IONICON PTR-MS for the same group of compounds.

We agree that including more data points would be valuable, but in this case adding more data from the conventional IONICON PTR-MS would not give additional information. We show that for 2-tridecanone (log C^0~5) the response is almost identical to that of the EVR-type instrument. Since the instrumental response time is already very close to the volumetric exchange time of the drift tube, we refrained from studying shorter-chain and thus more volatile ketones. We also show that for *cis*-pinonic acid (log C^0~3) τ_{90} is close to 2000 s for the conventional PTR-ToF-MS instrument, meaning that the three SVOCs we studied with the EVR-type instrument are simply not measureable with a conventional analyzer. It would certainly be interesting to compare the performance in the $3 < \log C^0 < 5$ range, but there we do not have any data (except for glycolic acid) and it would become a disproportionate effort to perform additional measurements study with two instruments.

9. Figure 4: I agree with the Referee 1 that operational temperatures should be clearly stated in the legend of this figure.

We have included the operational temperatures in the legend.

10. Figure 6: The authors state that mass concentrations of observed compounds were calculated under the assumption that all of these compounds were detected at the collisional rate. The authors should clarify how this collisional rate was calculated. In addition, they should explicitly mention it in the text as this is a fairly important assumption and can strongly affect the authors' conclusion about mass yields of observed compounds.

This figure has been moved to the Supplement and we provide additional details in the figure caption.

11. Conflict of interest: I agree with the Referee 1 that the authors should mention the fact that IONICON has been advertising the EVR PTR-MS setup for quite some time now.

We are now explicitly stating that IONICON Analytik commercializes PTR-MS, CHARON and EVR.

Technical corrections:

1. Line 307: remove "in an"

Done.

Introducing the Extended Volatility Range Proton-Transfer-Reaction Mass Spectrometer (EVR PTR-MS)

Felix Piel[1,2,+], Markus Müller[1], Klaus Winkler[1], Jenny Skytte af Sätra[3,*] and Armin Wisthaler[2,3]

[1] IONICON Analytik, Innsbruck, Austria
[2] Institute for Ion Physics and Applied Physics, University of Innsbruck, Innsbruck, Austria
[3] Department of Chemistry, University of Oslo, Oslo, Norway
[+] Now at: Department of Chemistry, University of Oslo, Oslo, Norway
[*] Now at: Norwegian Environment Agency, Oslo, Norway

Correspondence to: Armin Wisthaler (armin.wisthaler@kjemi.uio.no)

Abstract. Proton-transfer-reaction mass spectrometry (PTR-MS) is widely used in atmospheric sciences for measuring volatile organic compounds in real time. In the most widely used type of PTR-MS instruments, air is directly introduced into a chemical ionization reactor via an inlet capillary system. The reactor has a volumetric exchange time of ~0.1 s enabling PTR-MS analyzers to measure at a frequency of 10 Hz. The time response does, however, deteriorate if low-volatility analytes interact with surfaces in the inlet or in the instrument. Herein, we present the "Extended Volatility Range" (EVR) PTR-MS instrument which mitigates this issue. In the EVR configuration, inlet capillaries are made of passivated stainless steel and all wetted metal parts in the chemical ionization reactor are surface-passivated with a functionalized hydrogenated amorphous silicon coating. Heating the entire set-up (up to 120°C) further improves the time-response performance.

We carried out time-response performance tests on a set of 29 analytes having saturation mass concentrations C^0 in the range between 10^{-3} and 10^5 µg m^{-3}. 1/e-signal decay times after instant removal of the analyte from the sampling flow were between 0.2 and 90 s for gaseous analytes. We also tested the EVR PTR-MS instrument in combination with the CHARON particle inlet, and 1/e-signal decay times were in the range between 5 and 35 s for particulate analytes. We show on a set of exemplary compounds that the time-response performance of the EVR PTR-MS instrument is comparable to that of fastest flow tube chemical ionization mass spectrometers that are currently in use. The fast time response can be used for rapid (~ 1 min equilibration time) switching between gas and particle measurements. The CHARON EVR PTR-MS instrument can thus be used for real-time monitoring of both gaseous and particulate organics in the atmosphere. Finally, we show that the CHARON EVR PTR-MS instrument ~~is capable of detecting~~also rapidly detects highly oxygenated species (with up to eight oxygen atoms) in particles formed by limonene ozonolysis.

1 Introduction

The Earth's atmosphere contains a plethora of organic compounds, both in the gas and in the particulate phase (Goldstein and Galbally, 2007). Atmospheric organic compounds vary widely in their physico-chemical properties (*e.g.*, volatility, polarity, solubility), which makes their comprehensive measurement challenging (Heald and Kroll, 2020).

Proton-transfer-reaction mass spectrometry (PTR-MS) is widely used in atmospheric sciences for measuring volatile organic compounds (Hansel et al., 1995; de Gouw and Warneke, 2007; Yuan et al., 2017). In PTR-MS, air is directly introduced into an ion-molecule reactor wherein organic molecules ionize in collisions with hydronium (H_3O^+) ions. An electric field is applied across the ion-molecule-reactor, which is thus commonly referred to as the drift tube. Reagent and analyte ions are extracted from the drift tube and analyzed in a mass spectrometer.

One of the main advantages of PTR-MS is its rapidness. The drift tube has a volumetric exchange time of ~0.1 s enabling PTR-MS analyzers to measure at a frequency of 10 Hz (Müller et al., 2010). The time response does, however, deteriorate if low-volatility analytes interact with surfaces in the inlet or in the instrument. PTR-MS users have mitigated this problem by i) operating the drift tube at elevated temperature (Mikoviny et al., 2010), ii) increasing the flow through the drift tube (Breitenlechner et al., 2017; Krechmer et al., 2018) and iii) minimizing the wall collisions of analyte molecules (Breitenlechner et al., 2017). The problem of analyte adsorption becomes even more pronounced when particles are analyzed with the *Chemical Analysis of Aerosols Online* (CHARON) inlet (Eichler et al., 2015; Müller et al., 2017). After particle vaporization, low-volatility gases adsorb onto surfaces in the vaporizer, in the transfer line from the vaporizer to the drift tube and in the drift tube itself. This slows down the instrumental response significantly (Piel et al., 2019).

A second major advantage of PTR-MS is that H_3O^+ ion chemistry ~~s protonate~~detects a wide spectrum of organic analytes, ~~including both~~from non-oxidized to highly~~and~~ oxidized species~~organic analytes with similar and high efficiency. H_3O^+ ion chemistry thus detects a wider spectrum of analytes than any other chemical ionization method for atmospheric organic carbon~~. It must, however, be ensured that the analyte molecules ~~do~~ reach the ionization region and are not lost in the inlet line (*e.g.* Pagonis et al., 2017; Deming et al., 2019) or onto the drift tube walls~~ before ionization.~~

~~. If a long, low-flow and unheated polytetrafluoroethylene (PTFE) inlet line is used, the erroneous conclusion may be drawn that PTR-MS analyzers only detect singly and doubly oxygenated organic species (Riva et al., 2019).~~

Herein we will demonstrate how the use of heated inlet capillaries made of passivated stainless steel (SS) and of a heated ~~the passivation of all wetted~~ drift tube with passivated metal ~~parts~~ surfaces significantly ~~in the drift tube~~ improves the time response performance of PTR-MS analyzers. We will show that the heated and ~~have observed a~~passivated instrument ~~significantly improved measurement performance for~~time ~~responds fast~~se to low-volatility analytes, both ~~when measuring~~for ~~gas-phase~~es and particle-phase measurements~~s~~. The instrument set-up described herein has thus been named "*Extended Volatility Range*" (EVR) configuration.

2 Experimental

2.1 The EVR PTR-MS instrument

The PTR-MS instrument has been described in detail elsewhere (Yuan et al., 2017; and references therein). The data presented herein were obtained with two state-of-the-art CHARON PTR-MS analyzers (models PTR-TOF 4000X2 and PTR-TOF 6000X2) produced by Ionicon Analytik (Innsbruck, Austria). In their conventional set-up, these analyzers include inlet capillaries made of polyether ether ketone (PEEK) and a drift tube plus ion funnel consisting of electropolished SS drift rings and polytetrafluoroethylene (PTFE) spacers. PEEK and especially SS are known to adsorb certain analytes. In an effort to optimize the instrumental time response, we have eliminated all surfaces that are prone to analyte adsorption (Fig. 1). All ~~replaced all~~ PEEK capillaries were replaced by surface-treated SS capillaries. The surface treatment consisted ~~SS capillaries~~

~~were subject to a metal surface passivation~~in an application of ~~process in which a~~ functionalized hydrogenated amorphous silicon coating ~~is applied for minimizing analyte surface interactions~~. The same surface passivation was ~~also~~ applied to all wetted SS parts in the drift tube. In the CHARON inlet, the sampler and the vaporizer as well as ~~nd~~ the transfer tube from the vaporizer to the drift tube were surface-passivated. Fig. 1 shows all surface-treated parts in blue. As for conventional PTR-MS analyzers, the drift tube and inlet lines ~~is whole set up wase~~are housed in a temperature-controlled enclosure that can be operated ~~The inlet capillary and drift tube temperature (T_{drift}) can be varied~~ from room temperature to 120°C. The enclosure temperature is referred to as the drift tube temperature (T_{drift}).

2.2 Performance assessment of the EVR PTR-MS instrument

A laboratory study was carried out to measure signal decay times in the EVR PTR-MS analyzer for 29 analytes listed in the Supplement (Tab. S1). A single analyte was supplied in steady concentration to the analyzer and instantly ~~switched off~~removed from the inlet. $\tau_{1/e}$ is the time it took the analyte signal to decay to 1/e (36.8%) of its initial value. τ_{90} is the time it took the analyte signal to decay to ~~1/e (10%)~~ of its initial value~~$\tau_{1/e}$ was measured as the time that evolved until the analyte signal decayed to 36% of the initial stable signal intensity. τ_{90} was measured as the time that evolved until the signal decayed to 10% of the initial value~~. A stable gaseous analyte concentration, which is herein denoted with the subscript (g), was generated by placing a spatula tip of the solid sample into a 100 ml glass vial. The vial was heated and flushed with zero air (RH ~ 30%). Heating temperatures ranged from 50 to 120°C, depending upon the melting point of the analyte. The dynamic headspace of the vial was sampled through the gas inlet of the PTR-MS analyzer. Instrument and inlet were zeroed by overflowing the inlet with zero air (Fig. S1). A stable particulate analyte concentration, which is herein denoted with the subscript (p), was generated by dissolving an aliquot of the solid sample in HPLC-grade water (Sigma-Aldrich Chemie GmbH, Taufkirchen, Germany). The solution was then nebulized with a home-built nebulizer. The nebulizer outflow was dried with two home-built diffusion dryers and gases were removed with an activated charcoal denuder (NovaCarb F, Mast Carbon International Ltd., Guilford, UK). The CHARON inlet and PTR-MS instrument were zeroed by diverting the sample flow through a high efficiency particulate air (HEPA) filter (Fig. S1).

Exemplary data from a field study were taken to show the signal response of the EVR PTR-MS analyzer when switching between the CHARON particle inlet and the gas inlet. The data were collected during a measurement campaign at the TROPOS Research Station Melpitz (Spindler et al., 2013) in Germany in February 2019.

A laboratory study was carried out for investigating the capability of the CHARON EVR PTR-MS analyzer to detect highly oxidized organic molecules in particles. For this purpose, we reacted ozone and limonene in a flow reactor to form secondary organic aerosol (SOA). The reactor outflow was passed through an activated charcoal denuder (NovaCarb F, Mast Carbon International Ltd., Guilford, UK) for removing gaseous organics and subsequently injected into a 210 l steel barrel (Wilai GmbH, Wiedemar, Germany). The CHARON EVR PTR-MS analyzer sampled from this reservoir. The instrument was ~~with optimized instrumental settings (EVR, T_{drift} = 120°C). In addition, we~~ operated ~~the instrument~~ at low reduced electric field strength (E/N = 30 Td; 1 Td = 10^{-17} Vcm^{-2}) and with NH_4^+ as the reagent ion (Müller et al., 2020). With these instrumental settings, ionic fragmentation is largely suppressed and highly oxidized organic molecules ~~can be~~~~are~~are detected in their ammonium adduct form (Zaytsev et al., 2019~~Müller et al., in preparation~~).

3 Results and Discussion

3.1 ~~Signal decay in the~~Effect of surface passivation on time response ~~EVR PTR-MS instrument~~

Fig. 2~~1~~ shows data from two experiments wherein the signal decay of *cis*-pinonic acid$_{(g)}$ was measured with the same PTR-MS instrument, before and after being modified to the EVR configuration. T_{drift} was set to 100°C in both experiments; all other experimental parameters were also kept identical. In the conventional configuration, the analyte signal exhibited a long tailing while it rapidly dropped to near-zero levels in the EVR configuration. $\tau_{1/e}$ was 181 s for the conventional set-up and 4 s in the EVR configuration. These data clearly demonstrate that ~~the use of surface~~surface ~~passivated material~~passivation greatly improves the time response of PTR-MS analyzers.

Fig. 3 shows the response of the EVR PTR-MS analyzer (T_{drift} = 120°C) to an exemplary set of analytes, measured via the gas inlet (upper panel) and via the CHARON particle inlet (lower panel). ~~shows the signal decay in an EVR PTR-MS analyzer (T_{drift} = 120°C) after a steady supply of analyte was instantly switched off at t = 0 s. The upper panel shows exemplary data obtained for three gaseous analytes that were measured in separate experiments. The initial steady state mixing ratios are reported in the figure legend.~~ 4-nitrocatechol$_{(g)}$ (in dark yellow) exhibited a rather slow decay ($\tau_{1/e}$ = 27 s)~~,~~, *cis*-P~~p~~inonic acid$_{(g)}$ (in red) decayed in a few seconds ($\tau_{1/e}$ = 2.4 s)~~t $\tau_{1/e}$.~~ For ~~), and~~ 2-tridecanone (in blue), ~~dropped almost instantly to zero ($\tau_{1/e}$~~ was ~~=~~ 0.3 s~~). For, t~~which is ~~he latter, $\tau_{1/e}$ was~~ close to the volumetric exchange time of the drift tube (~ 0.1 s). The three exemplary compounds shown here cover the full three orders of magnitude span in $\tau_{1/e}$ (10^{-1} to 10^{2} s) that was observed for gaseous analytes. For particulate analytes, $\tau_{1/e}$ ranged from a few seconds to a few tens of seconds. The lower panel of Fig. 3~~1~~ shows exemplary data obtained for 2,7-dihydroxynaphthalene$_{(p)}$ (in dark yellow; $\tau_{1/e}$ = 15 s), levoglucosan$_{(p)}$ (in red; $\tau_{1/e}$ = 8.1 s) and nitrate$_{(p)}$ (in blue; $\tau_{1/e}$ = 4.4 s). The nitrate$_{(p)}$ signal originated from ammonium nitrate particles.

Fig. 4~~2~~ summarizes the $\tau_{1/e}$ values measured for 21 gaseous analytes (upper panel) and 15 particulate analytes (lower panel).

The color-coding and sizing are explained in the figure legend. Mixing ratios were quantified according to the procedure outlined in the Supplement of Müller et al. (2017) and were typically in the 0.1–10 ppbv range. For some compounds ~~Higher levels (up to 100 ppbv) were only used for a few compounds~~ (vanillin$_{(g)}$, 2-tridecanone$_{(g)}$, 2,6-dimethoxyphenol$_{(g)}$, 4-nitroguaiacol$_{(g)}$, ammonia$_{(g)}$) it was difficult to generate mixing ratios in the low-ppbv range, which is why we also included mixing ratios up to 100 ppbv ~~are reported~~in our analysis. We typically measured $\tau_{1/e}$ at three different mixing ratios for each compound. Since these were in a rather narrow range, only small changes in the instrumental time response were observed. We will thus not discuss any concentration dependence of $\tau_{1/e}$ here. We observed an increase in $\tau_{1/e}$ with decreasing saturation mass concentrations (log C^0) as a general trend, although with significant deviations for some compounds (Fig. S2). Glucose$_{(g)}$, for example, exhibited a much faster response than the sugar alcohols (xylitol$_{(g)}$, arabitol$_{(g)}$) despite having a similar log C^0. Structural effects may play a role here, since glucose is a cyclic molecule, while the sugar alcohols are both linear. It is also important to note that the SIMPOL.1 method has not been validated for saccharides and that the calculated log C^0 may be inaccurate. 4-nitrocatechol, with a relatively high log C^0 of 4.2, was among the slowest responding gaseous analytes. This observation remains unexplained. With the CHARON inlet connected, $\tau_{1/e}$ was in the 5 to 20 s range for most analytes (Fig. 4~~2~~, lower panel). Exceptions were diglycolic acid$_{(p)}$ and tartaric acid$_{(p)}$ with $\tau_{1/e}$ up to ~35 s. Notably, no obvious dependence of $\tau_{1/e}$ on log C^0 was observed. Levoglucosan, 2,7-dihydroxynaphthalene, stearic acid, azelaic acid, diglycolic acid and vanillic acid were studied in both phases. The instrumental response was typically ~5 s slower in the particle measurements. The CHARON inlet has a larger surface area and a lower sample flow than the gas inlet. Stearic acid and azelaic acid responded faster with the CHARON inlet, which remains unexplained. The reader is cautioned that the $\tau_{1/e}$ values presented in Fig. 4~~2~~ should not be taken as absolute and generally applicable values. The reported numbers should be seen as indicative estimates

for the time response of state-of-the-art IONICON EVR PTR-MS instruments. It is well known that analytes compete for surface adsorption with other matrix constituents such as water or other surface-affine compounds. All of our experiments were carried out with a single compound at one humidity level. We consider it beyond the scope of this work to investigate a matrix dependence of $\tau_{1/e}$. In previous work, we anecdotally observed that basic analytes exhibited a significantly slower time response when acidic samples had been sampled before. The sampling history was not considered in our study.

3.2 Drift tube temperature effects

For long-chain ketones (Pagonis et al., 2017; Krechmer et al., 2018) and carboxylic acids (Fig. S2), $\tau_{1/e}$ exhibits the expected increase with decreasing log C^0. Since log C^0 depends upon temperature, changes in ~~We investigated the effect of~~ T_{drift} should lead to predictable changes in $\tau_{1/e}$. We thus measured ~~on~~ $\tau_{1/e}$ for ~~two gaseous analytes,~~ 2-tridecanone$_{(g)}$ and *cis*-pinonic acid$_{(g)}$ at variable T_{drift} (Fig. ~~5~~3). In the case of 2-tridecanone$_{(g)}$ (upper panel), an increase in T_{drift} from room temperature to 60 °C decreased $\tau_{1/e}$ from 24 s to 2 s. At T_{drift} = 100°C, $\tau_{1/e}$ was 0.3 s approaching the volumetric exchange time of the drift tube. In the case of *cis*-pinonic acid$_{(g)}$ (lower panel), we only investigated ~~the 80 to 120°C~~ temperatures of 80°C and ~~range~~ above because the solid analyte sample was kept at 70°C. When increasing T_{drift} from 80 to 120°C, ~~in which~~ $\tau_{1/e}$ dropped from 6.5 to 2.4 s. For the two compounds investigated, the decrease in $\tau_{1/e}$ can be explained by the increase in log C^0 with temperature. According to Epstein et al. (2010), a 15°C temperature rise increases log C^0 by ~1 in the 0 to 50°C temperature range. The effect becomes less pronounced at higher temperatures. For *cis*-pinonic acid, the SIMPOL.1 method yields a log C^0 increase from 5.2 to 6.2 in the 80 to 120°C temperature range. At 45°C, 2-tridecanone has roughly the same log C^0 as *cis*-pinonic acid at 120°C (Fig. S3). Consistently, we observed a similar time response for the two compounds at T_{drift} = 45°C and T_{drift} = 120°C, respectively. We conclude that increasing T_{drift} to 120°C is an effective way for reducing $\tau_{1/e}$ in EVR PTR-MS analyzers.

Exposing the sample gas to heated surfaces ~~elevated temperatures~~ in an analyzer, may thermally degrade some ~~of the~~ analytes. It is important to note that none of t~~Importantly,~~ he acids studied in this work decarboxylated at T_{drift} = 120°C. It may, however, be necessary to use a lower T_{drift} when more thermally labile ~~thermally more labile~~ analytes are targeted.~~ none of the compounds studied herein thermally decomposed at this temperature. This needs to be carefully assessed when a higher T_{drift} is used or when thermally labile compounds are to be analyzed.~~

3.3 Response times of different online CIMS instruments

Fig. 6~~4~~ compares the signal decay times (here reported as τ_{90} and not as $\tau_{1/e}$) as observed in~~of~~ different online CIMS instruments~~ to a set of ketones, carboxylic acids and hydroxycarbonyls in the gas phase.~~ The plot includes data from this study, which were obtained with two state-of-the-art IONICON PTR-MS analyzers. The data points in yellow were obtained with a conventional instrument, while the data points in dark red were collected with an EVR-type analyzer. Both instruments were operated at T_{drift} = 120°C. The figure also includes literature data obtained with an old quadrupole PTR-MS instrument (qPTR-MS; in blue: Pagonis et al., 2017), with a PTR-ToF-MS analyzer from a different manufacturer (VOCUS^{TM}; in orange: Krechmer et al., 2018) and with two iodide (I^-) CIMS instruments (in green: Liu et al., 2019; in light blue: Palm et al., 2019), respectively. The latter four instruments were all operated at room temperature. ~~-~~τ_{90} is plotted against log C^0 of the respective analyte~~, (specified on the upper horizontal axis)~~ which was calculated using the SIMPOL.1 method (Pankow and Asher, 2008). The upper horizontal axis lists the compound names; the lower horizontal axis shows in which log C^0 range molecules are classified as volatile organic compounds (VOCs), intermediate volatility organic compounds (IVOCs) and semi-volatile organic compounds (SVOCs). Since the instruments did not measure the same SVOCs, we only use our carboxylic acid data for the log C^0-based comparison. For the acids, log C^0 appears to be the main determinant of τ_{90} while for the saccharides and substituted phenols other properties affect τ_{90} (Fig. S2). For VOCs and the more volatile IVOCs (log $C^0 \geq 5$), τ_{90} is close to the volumetric exchange time of the drift tube for both the EVR and the conventional PTR-ToF-MS instrument, if the drift tube

and inlet are heated to 120 °C. Conventional unheated PTR-MS instruments have a much slower time response. For the less volatile IVOCs (log $C^0 \leq 3$; *cis*-pinonic acid) surface passivation reduces τ_{90} by two orders of magnitude, even if the drift tube is heated to 120 °C in both the conventional and the EVR PTR-ToF-MS analyzer. For the SVOCs, the heated EVR PTR-ToF-MS has a similar time response as ~~At T_{drift} = 120°C, even the conventional PTR-MS analyzer responded almost instantly to C_7, C_{10} and C_{13} ketones. For the C_{13} species, the EVR-type instrument responded only ~20% faster than the conventional analyzer. The VOCUS™ instrument and the qPTR-MS analyzer exhibited a much slower response to these ketones. We explain this by the fact that both of these instruments were operated at room temperature.~~

~~The superior performance of the EVR-type instrument becomes evident when measuring carboxylic acids. In the case of *cis*-pinonic acid$_{(g)}$, τ_{90} decreased by a factor of 30 when using an EVR PTR-MS analyzer instead of a conventional instrument. Stearic, azelaic and diglycolic acid, for which log C^0 ranges roughly from 1 to 2, exhibited response times in the range of 1 to 2 minutes. This is as fast as~~ an optimized I^- CIMS instrument with reduced instrument wall interactions ~~responded to dihydroxycarbonyls with a log C^0 ~2~~ (Palm et al., 2019). ~~A significantly slower response was recently reported for another I^- CIMS instrument (Liu et al., 2019).~~

3.4 Rapid switching between the gas inlet and the CHARON particle inlet

For certain applications~~,~~ it is desirable to periodically switch between ~~the~~ gas and particle measurements. Fig. 7~~5~~ shows exemplary data collected by a CHARON EVR PTR-MS instrument during ambient air measurements at a rural background station in Germany.

The reader should focus on the transition from background to ambient particle measurements at 06:15:40 and the transition from particle to gas measurements at 06:21:40, which is when the slow signal response becomes most evident. The upper panel shows the time evolution of the NH_4^+ (*m/z* 18.034) and NO_2^+ (*m/z* 45.996) signals. In the CHARON inlet, ammonium nitrate particles evaporate to yield gaseous ammonia (NH_3) and nitric acid (HNO_3). Ammonia is detected in its protonated form, while protonated nitric acid dehydrates upon protonation to yield the nitronium ion (NO_2^+). Both ammonia and nitric acid are particularly prone to adsorptive losses on stainless steel (Neuman et al., 1999; Nowak et al., 2007). In the EVR-type instrument, wetted surfaces do not include any untreated stainless steel, which results in a fast instrumental response to both compounds. Both the NH_4^+ and the NO_2^+ signal equilibrated within 1 minute when switching from HEPA to ambient CHARON measurements and from particle to gas measurements, respectively. The lower panel shows the evolution of the $C_4H_5O^+$ (m/z 69.033) and $C_6H_9O_4^+$ (m/z 145.049) signals within one measurement cycle. $C_6H_9O_4^+$ is the main ionic fragment from levoglucosan (Leglise et al., 2019). $C_4H_5O^+$ is believed to be a fragment of larger furanoid compounds in particles and protonated furan in the gas measurement. The instrumental response to these analytes was somewhat slower than to ammonium nitrate but equilibration still occurred within 1 minute. The instrumental response to levoglucosan is similar to what we observed in single compound measurements in the laboratory, suggesting that the presence of a complex matrix does not negatively affect instrumental response times.

3.5 Detection of highly oxidized organic compounds

The CHARON PTR-MS instrument has been successfully used for measuring the chemical composition of SOA (*e.g.*, Gkatzelis et al., 2018). The detection of highly oxidized~~such~~ species ~~by CHARON PTR-MS~~ has, however, ~~hitherto~~ been hampered by the adsorption of low-volatility species onto instrumental surfaces. ~~highly oxidized molecules onto SS surfaces in the instrument.~~ In an ~~effort~~ attempt to demonstrate~~test~~ the improved detection capability of the CHARON EVR PTR-MS instrument ~~capability of detecting highly oxidized species~~, we ~~measured~~ sampled SOA generated from limonene ozonolysis. Up to eight oxygen atoms were detected in the analyte ions ~~– with optimized instrumental settings (EVR, T_{drift} = 120°C). In addition, we operated the instrument at low reduced electric field strength (E/N = 30 Td; 1 Td = 10^{-17} Vcm^{-2}) and with NH_4^+~~

~~as the reagent ion (Müller et al., 2020). With these instrumental settings, ionic fragmentation is largely suppressed and highly oxidized organic molecules are detected in their ammonium adduct form (Müller et al., in preparation).~~

~~Fig. S2~~ure 6 shows the normalized mass distribution of oxidized species detected in limonene/O_3 ~~SOA as a function of #O, which ranged from 1 to~~ (Fig S~~2~~4)~~8~~. Fig. ~~9~~8 shows the rapid decay ($\tau_{1/e}$ = 1~~3~~5 s) of an O_8-compound (~~the~~ $C_{19}H_{30}O_8$ detected as ammonium adduct)~~ compound~~ when~~-~~ switching~~ing~~ from the CHARON particle inlet to the gas inlet. The rapidness of the decay suggests that surface adsorption effects play a minor role even for such highly oxidized species. Hammes et al. (2019) claimed that~~assign~~ the $C_{19}H_{30}O_8$ molecule formed from limonene ozonolysis is a multifunctional compound containing three keto groups, one carboxyl group, one hydroperoxy group and one ester group. A calculation using SIMPOL.1 (Pankow and Asher, 2008) yields a log C^0 of -5.9 for this molecule, suggesting that even extremely low-volatility organic compounds (ELVOCs) can be monitored in real time by CHARON EVR PTR-MS. ~~. Hammes et al. (2019) assign this molecular formula to a hydroperoxide, for which we calculate a logC0 of -5.9. This would suggest that the CHARON EVR PTR-MS instrument is capable of detecting ELVOCs, although this warrants further investigation.~~

The fact that the detected $C_{19}H_{30}O_8$ molecule contains a ~~may be a~~ hydroperoxy group is notable~~ide is interesting~~, because hydroperoxides are known to ~~The majority of the highly oxidized compounds (#O ≥ 3) are monomers (#C ≤ 10, ~55% of the total mass). The most abundant ions observed fall into this category and can be assigned to limonene ozonolysis products previously reported in the literature (Tab. S4). For the condensation products or dimers (#C > 10), ~7% of the total mass was composed of highly oxidized compounds. Compounds with #O > 6 were equally distributed between monomers and dimers. We detected compounds up to #O = 8, which accounted for ~ 0.5 % of the total measured mass concentration.~~

~~It is worth pointing out that some of the ions detected in limonene/O_3 SOA (Fig. S4) have been previously associated with analytes containing a hydroperoxy functional group . Rivera Rios et al. (2014) observed that hydroperoxides~~ efficiently decompose on ~~the~~ metal ~~parts (inlet, drift tube) of~~surfaces in conventional PTR-MS instruments (Rivera-Rios et al., 2014). An additional benefit of surface passivation may ~~the EVR configuration could~~ thus be that ~~o prevent~~ the metal-catalyzed decomposition of peroxides and hydroperoxides is suppressed. Preliminary laboratory tests with cumene hydroperoxide and dicumylperoxide (*i.e.*, the only peroxides that are commercially available, although with significant impurities) indicate that these compounds do indeed not decompose in ~~his process does not occur in~~ EVR-type instruments. ~~An additional benefit of the EVR configuration may thus be that the metal catalyzed decomposition of labile compounds (*e.g.*, peroxides and hydroperoxides) is eliminated or suppressed.~~ More work is needed to confirm this preliminary finding.

4 Conclusion

We have described and characterized the novel EVR PTR-MS instrument, which exhibits a significantly improved time-response performance as compared to conventional IONICON PTR-MS analyzers. The time response of this optimized instrument is comparable to that of fastest flow tube CIMS instruments that are currently in use. This allows to rapidly switch between gas and particle measurements, making the CHARON EVR PTR-MS instrument the only direct sample introduction CIMS instrument that can monitor gaseous and particulate organics in the atmosphere in real time. Besides being faster, the EVR PTR-MS instrument also allows to target new analyte classes such as highly oxygenated organic molecules and potentially also hydroperoxides. We believe that the CHARON EVR PTR-MS instrument will be a valuable tool for overcoming current challenges in the measurement of atmospheric organic carbon (Heald and Kroll, 2020).

Author contribution

KW developed the EVR system and performed initial tests. MM, FP and AW designed the experimental studies. MM, FP and JSS carried out the experiments. FP performed the data analysis, with support from JSS and MM. FP and MM drafted the manuscript. AW wrote the final manuscript. All authors commented and accepted the final version of the manuscript.

Conflicts of interest

MM, FP and KW work for IONICON Analytik. ~~,~~ IONICON Analytik ~~which is~~ commercializes~~zing~~ ~~(CHARON)~~ PTR-MS instruments (both in the conventional and in the EVR configuration) and the CHARON particle inlet. MM and AW profit from a license agreement (CHARON inlet) between the University of Innsbruck and IONICON Analytik.

Acknowledgements

We like to thank Laurent Poulain and Gerald Spindler from TROPOS for their support during the measurements in Melpitz. Measurements in Melpitz were supported by the European Union's Horizon 2020 research and innovation programme under grant agreement N°654109 (ACTRIS-2). FP has received funding from the European Union's Horizon 2020 research and innovation programme under grant agreement N°674911 (IMPACT). Special thanks go to Magda Claeys for providing many of the substances studied in this work.

References

Breitenlechner, M., Fischer, L., Hainer, M., Heinritzi, M., Curtius, J. and Hansel, A.: PTR3: An Instrument for Studying the Lifecycle of Reactive Organic Carbon in the Atmosphere, Anal. Chem., 89(11), 5824–5831, doi:10.1021/acs.analchem.6b05110, 2017.

Deming, B. L., Pagonis, D., Liu, X., Day, D. A., Talukdar, R., Krechmer, J. E., de Gouw, J. A., Jimenez, J. L. and Ziemann, P. J.: Measurements of delays of gas-phase compounds in a wide variety of tubing materials due to gas–wall interactions, Atmos. Meas. Tech., 12(6), 3453–3461, doi:10.5194/amt-12-3453-2019, 2019.

Eichler, P., Müller, M., D'Anna, B. and Wisthaler, A.: A novel inlet system for online chemical analysis of semi-volatile submicron particulate matter, Atmos. Meas. Tech., 8(3), 1353–1360, doi:10.5194/amt-8-1353-2015, 2015.

Epstein, S. A., Riipinen, I. and Donahue, N. M.: A Semiempirical Correlation between Enthalpy of Vaporization and Saturation Concentration for Organic Aerosol, Environ. Sci. Technol., 44(2), 743–748, doi:10.1021/es902497z, 2010.

Goldstein, A. H. and Galbally, I. E.: Known and Unexplored Organic Constituents in the Earth's Atmosphere, Environ. Sci. Technol., 41(5), 1514–1521, doi:10.1021/es072476p, 2007.

de Gouw, J. and Warneke, C.: Measurements of volatile organic compounds in the earth's atmosphere using proton-transfer-reaction mass spectrometry, Mass Spectrom. Rev., 26(2), 223–257, doi:10.1002/mas.20119, 2007.

Hammes, J., Lutz, A., Mentel, T., Faxon, C. and Hallquist, M.: Carboxylic acids from limonene oxidation by ozone and OH radicals: Insights into mechanisms derived using a FIGAERO-CIMS, Atmos. Chem. Phys., 19(20), 13037–13052, doi: 10.5194/acp-19-13037-2019, 2019.

Hansel, A., Jordan, A., Holzinger, R., Prazeller, P., Vogel, W. and Lindinger, W.: Proton transfer reaction mass spectrometry: on-line trace gas analysis at the ppb level, Int. J. Mass. Spectrom., 149–150, 609–619, doi:10.1016/0168-1176(95)04294-U, 1995.

Heald, C. L. and Kroll, J. H.: The fuel of atmospheric chemistry: Toward a complete description of reactive organic carbon, Sci. Adv., 6(6), eaay8967, doi:10.1126/sciadv.aay8967, 2020.

Krechmer, J., Lopez-Hilfiker, F., Koss, A., Hutterli, M., Stoermer, C., Deming, B., Kimmel, J., Warneke, C., Holzinger, R., Jayne, J., Worsnop, D., Fuhrer, K., Gonin, M. and de Gouw, J.: Evaluation of a New Reagent-Ion Source and Focusing Ion–Molecule Reactor for Use in Proton-Transfer-Reaction Mass Spectrometry, Anal. Chem., 90(20), 12011–12018, doi:10.1021/acs.analchem.8b02641, 2018.

Leglise, J., Müller, M., Piel, F., Otto, T. and Wisthaler, A.: Bulk organic aerosol analysis by PTR-MS: an improved methodology for the determination of total organic mass, O:C and H:C elemental ratios and the average molecular formula, Anal. Chem., acs.analchem.9b02949, doi:10.1021/acs.analchem.9b02949, 2019.

Liu, X., Deming, B., Pagonis, D., Day, D. A., Palm, B. B., Talukdar, R., Roberts, J. M., Veres, P. R., Krechmer, J. E., Thornton, J. A., de Gouw, J. A., Ziemann, P. J. and Jimenez, J. L.: Effects of gas–wall interactions on measurements of semivolatile compounds and small polar molecules, Atmos. Meas. Tech., 12(6), 3137–3149, doi:10.5194/amt-12-3137-2019, 2019.

Mikoviny, T., Kaser, L. and Wisthaler, A.: Development and characterization of a High-Temperature Proton-Transfer-Reaction Mass Spectrometer (HT-PTR-MS), Atmos. Meas. Tech., 3(3), 537–544, doi:10.5194/amt-3-537-2010, 2010.

Müller, M., Graus, M., Ruuskanen, T. M., Schnitzhofer, R., Bamberger, I., Kaser, L., Titzmann, T., Hörtnagl, L., Wohlfahrt, G., Karl, T. and Hansel, A.: First eddy covariance flux measurements by PTR-TOF, Atmos. Meas. Tech., 3(2), 387–395, doi:10.5194/amt-3-387-2010, 2010.

Müller, M., Eichler, P., D'Anna, B., Tan, W. and Wisthaler, A.: Direct Sampling and Analysis of Atmospheric Particulate Organic Matter by Proton-Transfer-Reaction Mass Spectrometry, Anal. Chem., 89(20), 10889–10897, doi:10.1021/acs.analchem.7b02582, 2017.

Müller, M., Piel, F., Gutmann, R., Sulzer, P., Hartungen, E. and Wisthaler, A.: A novel method for producing NH4+ reagent ions in the hollow cathode glow discharge ion source of PTR-MS instruments, Int. J. Mass. Spectrom., 447, 116254, doi:10.1016/j.ijms.2019.116254, 2020.

Neuman, J. A., Huey, L. G., Ryerson, T. B. and Fahey, D. W.: Study of Inlet Materials for Sampling Atmospheric Nitric Acid, Environ. Sci. Technol., 33(7), 1133–1136, doi:10.1021/es980767f, 1999.

Nowak, J. B., Neuman, J. A., Kozai, K., Huey, L. G., Tanner, D. J., Holloway, J. S., Ryerson, T. B., Frost, G. J., McKeen, S. A. and Fehsenfeld, F. C.: A chemical ionization mass spectrometry technique for airborne measurements of ammonia: AIRBORNE CIMS NH $_3$ MEASUREMENTS, J. Geophys. Res., 112(D10), doi:10.1029/2006JD007589, 2007.

Pagonis, D., Krechmer, J. E., de Gouw, J., Jimenez, J. L. and Ziemann, P. J.: Effects of gas–wall partitioning in Teflon tubing and instrumentation on time-resolved measurements of gas-phase organic compounds, Atmos. Meas. Tech., 10(12), 4687–4696, doi:10.5194/amt-10-4687-2017, 2017.

Palm, B. B., Liu, X., Jimenez, J. L. and Thornton, J. A.: Performance of a new co-axial ion-molecule reaction region for low-pressure chemical ionization mass spectrometry with reduced instrument wall interactions, Atmos. Meas. Tech., 12(11), 5829–5844, doi:10.5194/amt-12-5829-2019, 2019.

Pankow, J. F. and Asher, W. E.: SIMPOL.1: a simple group contribution method for predicting vapor pressures and enthalpies of vaporization of multifunctional organic compounds, Atmos. Chem. Phys., 8(10), 2773–2796, doi:10.5194/acp-8-2773-2008, 2008.

Piel, F., Müller, M., Mikoviny, T., Pusede, S. E. and Wisthaler, A.: Airborne measurements of particulate organic matter by proton-transfer-reaction mass spectrometry (PTR-MS): a pilot study, Atmos. Meas. Tech., 12(11), 5947–5958, doi:10.5194/amt-12-5947-2019, 2019.

~~Riva, M., Rantala, P., Krechmer, J. E., Peräkylä, O., Zhang, Y., Heikkinen, L., Garmash, O., Yan, C., Kulmala, M., Worsnop, D. and Ehn, M.: Evaluating the performance of five different chemical ionization techniques for detecting gaseous oxygenated organic species, Atmos. Meas. Tech., 12(4), 2403–2421, doi:10.5194/amt-12-2403-2019, 2019.~~

Rivera-Rios, J. C., Nguyen, T. B., Crounse, J. D., Jud, W., St. Clair, J. M., Mikoviny, T., Gilman, J. B., Lerner, B. M., Kaiser, J. B., Gouw, J., Wisthaler, A., Hansel, A., Wennberg, P. O., Seinfeld, J. H. and Keutsch, F. N.: Conversion of hydroperoxides to carbonyls in field and laboratory instrumentation: Observational bias in diagnosing pristine versus anthropogenically controlled atmospheric chemistry, Geophys. Res. Lett., 41(23), 8645–8651, doi:10.1002/2014GL061919, 2014.

Spindler, G., Grüner, A., Müller, K., Schlimper, S. and Herrmann, H.: Long-term size-segregated particle (PM10, PM2.5, PM1) characterization study at Melpitz -- influence of air mass inflow, weather conditions and season, J. Atmos. Chem., 70(2), 165–195, doi:10.1007/s10874-013-9263-8, 2013.

Yuan, B., Koss, A. R., Warneke, C., Coggon, M., Sekimoto, K. and de Gouw, J. A.: Proton-Transfer-Reaction Mass Spectrometry: Applications in Atmospheric Sciences, Chem. Rev., 117(21), 13187–13229, doi:10.1021/acs.chemrev.7b00325, 2017.

Zaytsev, A., Breitenlechner, M., Koss, A.R., Lim, C. Y., Rowe, J. C., Kroll, J. H. and Keutsch, F. N.: Using Collision-Induced Dissociation to Constrain Sensitivity of Ammonia Chemical Ionization Mass Spectrometry (NH_4^+ CIMS) to Oxygenated Volatile Organic Compounds. Atmos. Meas. Tech., 12(3), 1861–1870, doi:10.5194/amt-12-1861-2019, 2019.

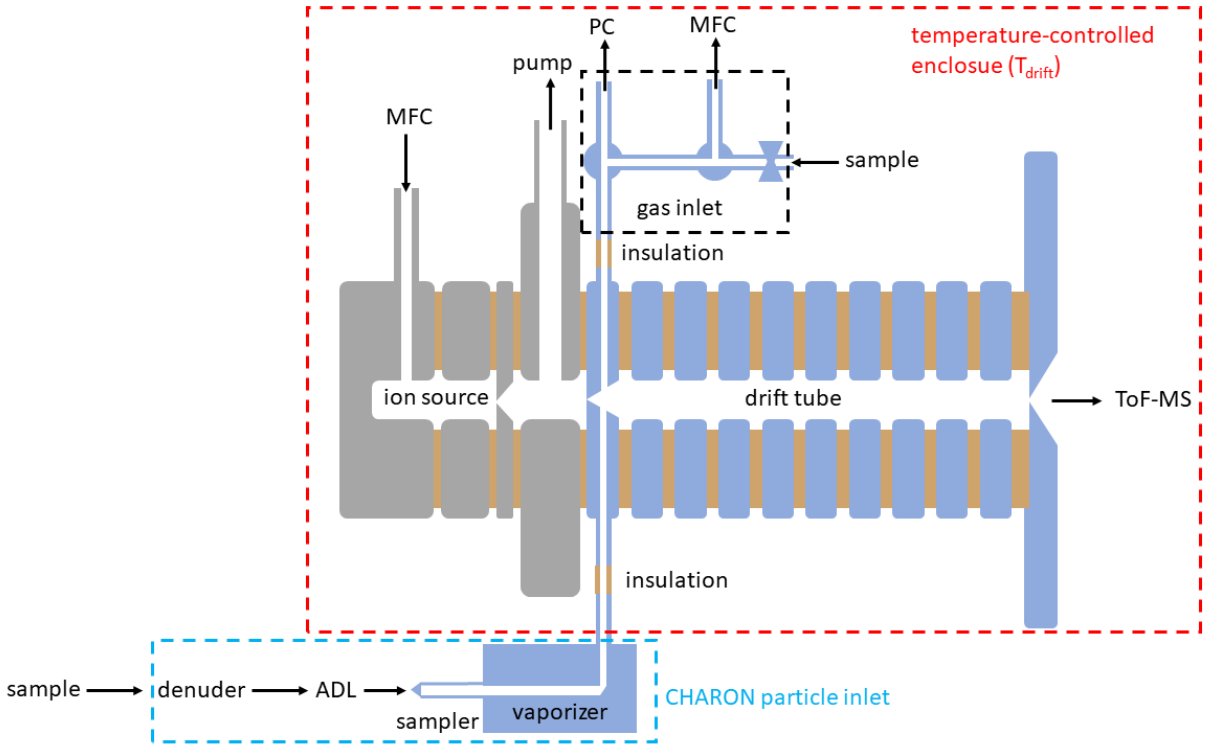

Figure 1. Scheme of the EVR PTR-MS instrument including a gas inlet and the CHARON particle inlet. The parts in blue were passivated with a functionalized hydrogenated amorphous silicon coating. MFC: mass flow controller; PC: pressure controller, ADL: aerodynamic lens; ToF-MS: time-of-flight mass spectrometer

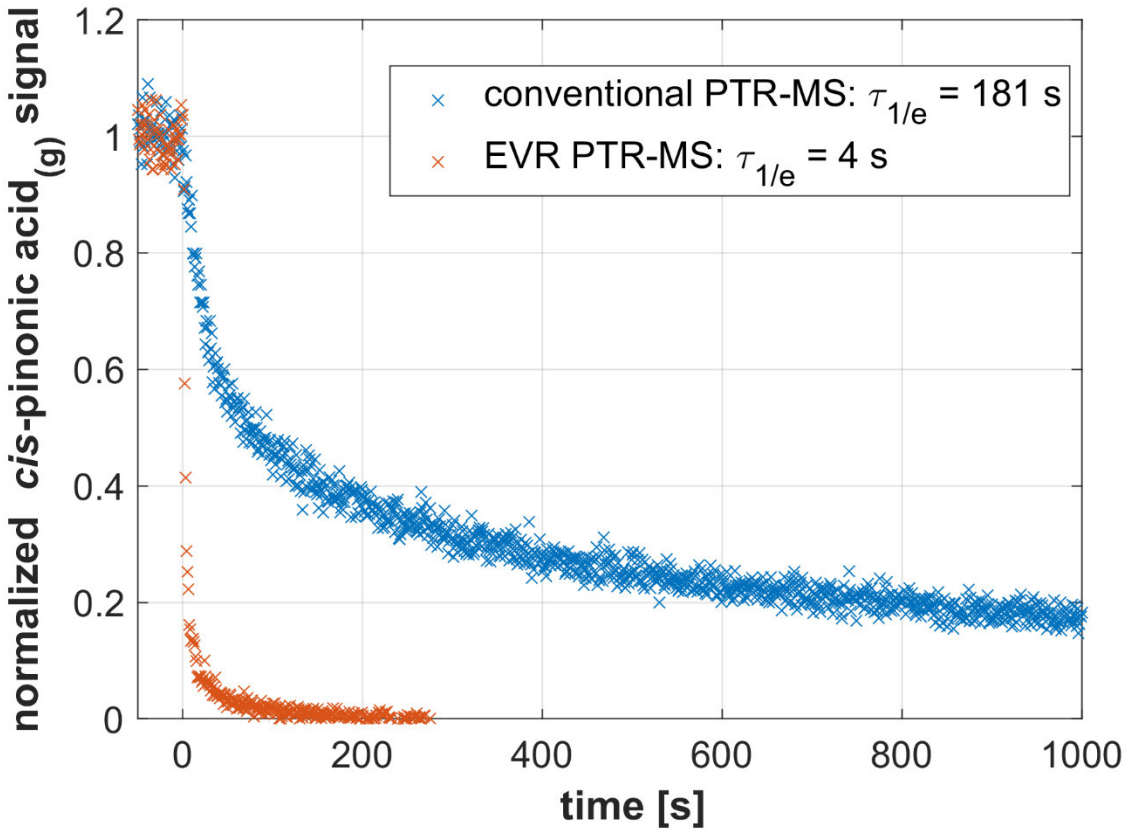

Figure 2. Signal decay as observed in a conventional PTR-MS instrument (T_{drift} = 120°C; in blue) and in an EVR PTR-MS analyzer (T_{drift} = 120°C; in red) after a steady supply of gaseous *cis*-pinonic acid was instantly switched off a t = 0 s.

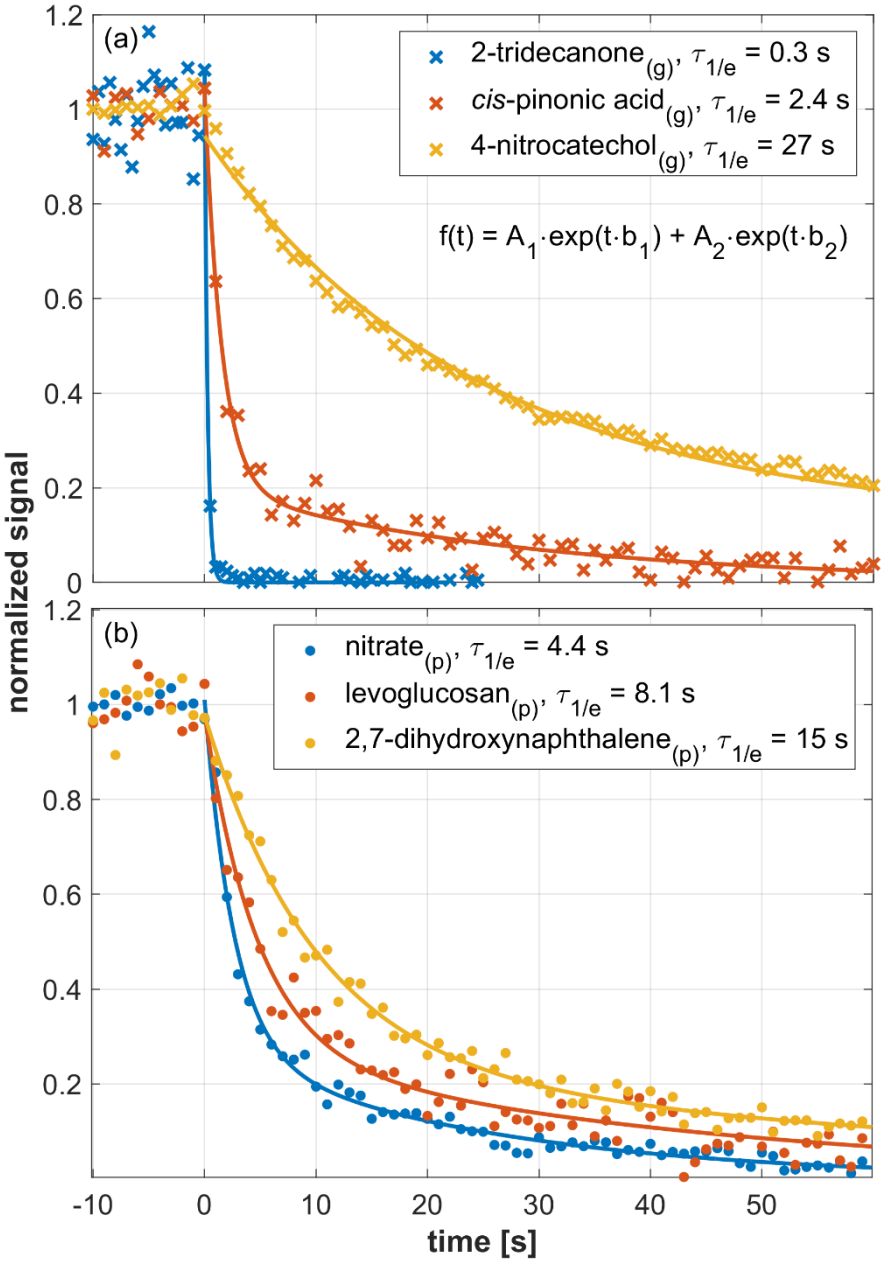

Figure ~~13~~. Signal decay as observed in an ~~in an~~ EVR PTR-MS analyzer (T_{drift} = 120°C) after a steady supply of analyte was instantly switched off a t = 0 s. The decay of gaseous analytes is shown in the upper panel, while the lower panel refers to particulate analytes. Initial steady-state mixing ratios were as follows: 2-tridecanone$_{(g)}$: 1 ppbv, *cis*-pinonic acid$_{(g)}$: 2.2 ppbv, 4-nitrocatechol$_{(g)}$: 30 ppbv, nitrate: 3 ppbv; levoglucosan$_{(p)}$: 1.2 ppbv, 2,7-dihydroxynaphtalene$_{(p)}$: 0.3 ppbv. Signals were fitted using a double exponential decay function (see insert in the upper panel). All fitting parameters are listed in Table S2.

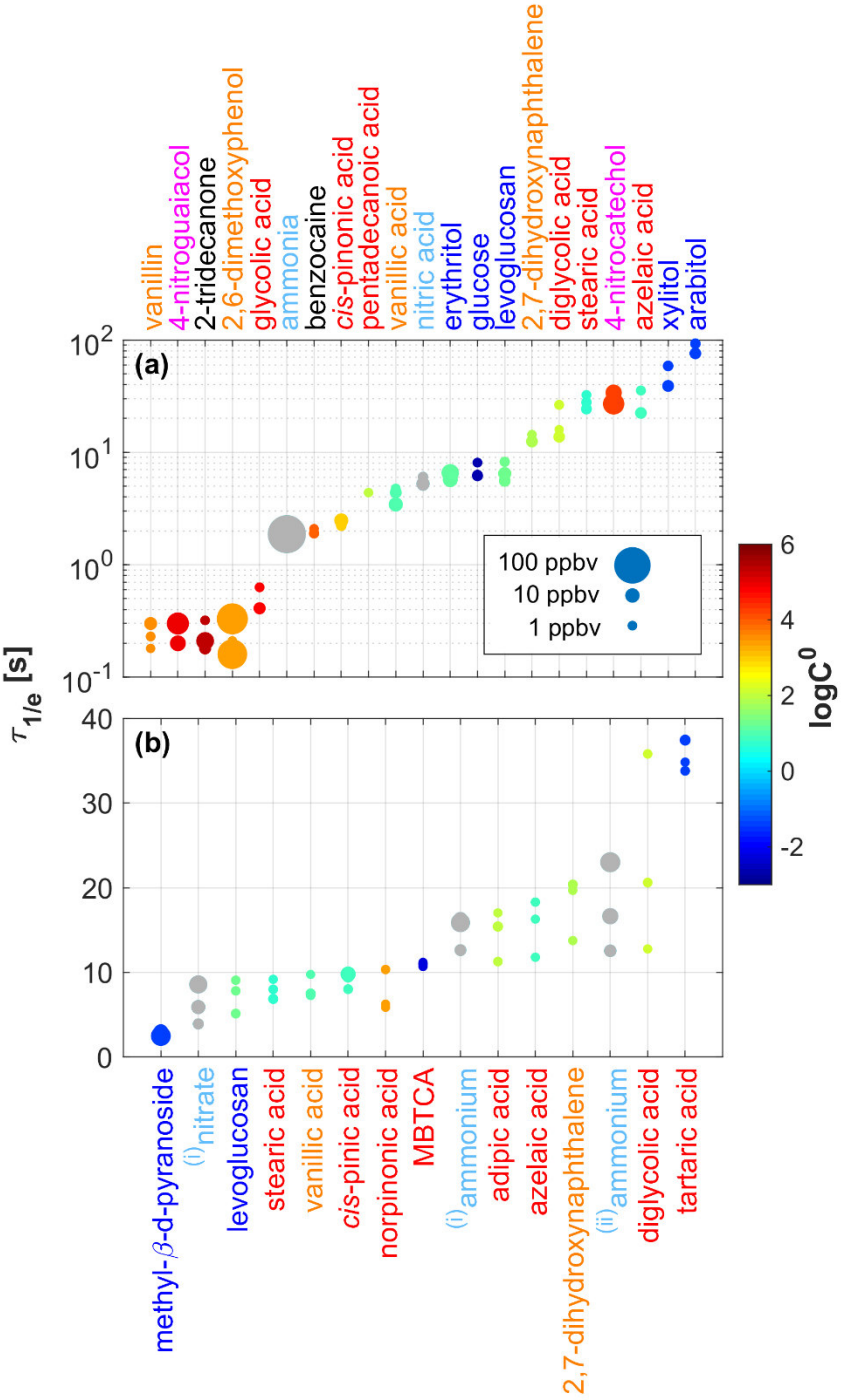

Figure ~~24~~. Signal decay times ($\tau_{1/e}$) measured for 21 gaseous analytes (upper panel) and 15 particulate analytes (lower panel). Analytes were grouped and color-coded into six classes: saccharides (in dark blue), carboxylic acids (in red), substituted phenols (in orange), nitroaromatics (in magenta), small polar molecules (in light blue) and others (in black). The size of the dots indicates the initial steady-state mixing ratio (0.1–100 ppbv) used in the respective experiment. The color code of the data points indicates the saturation mass concentrations (log C^0) of the analytes as calculated using the SIMPOL.1 method (Pankow and Asher, 2008).

(i) originating from ammonium nitrate, (ii) originating from ammonium sulfate

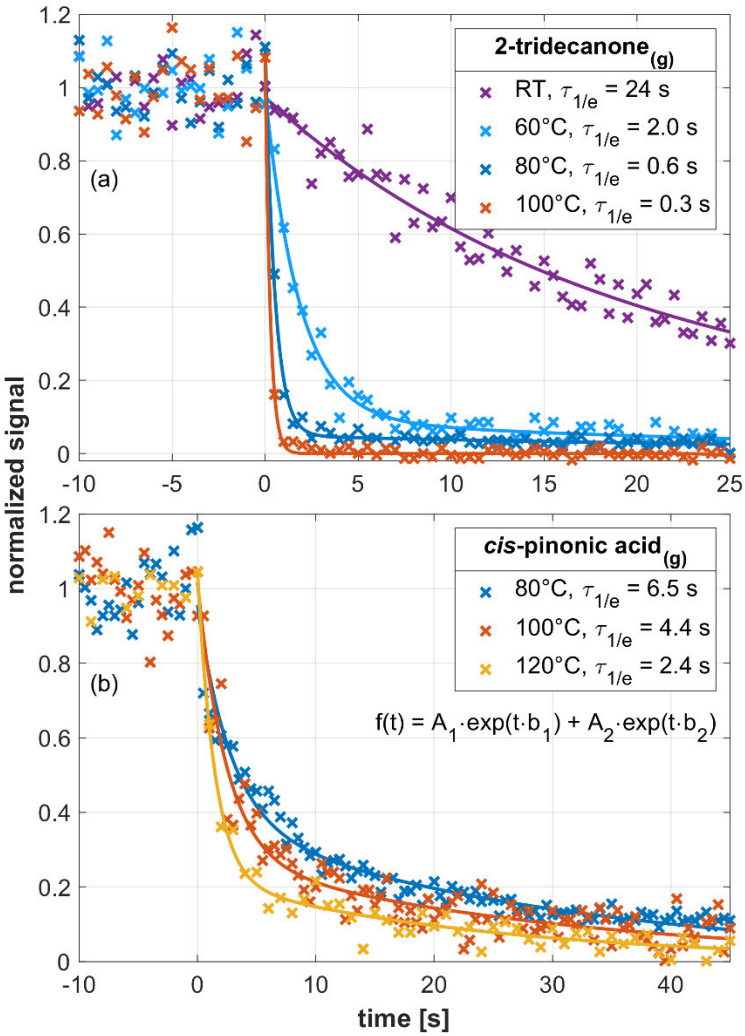

Figure ~~3~~5. Signal decay as observed in an EVR PTR-MS analyzer for 2-tridecanone$_{(g)}$ (upper panel)) and *cis*-pinonic acid$_{(g)}$, respectively, at different drift tube temperatures. Initial steady-state mixing ratios were as follows: 2-tridecanone$_{(g)}$: 1–1.3 ppbv; *cis*-pinonic acid: 2.2 ppbv. Signals were fitted using a double exponential decay function (see insert in the lower panel). All fitting parameters are listed in Table S3.

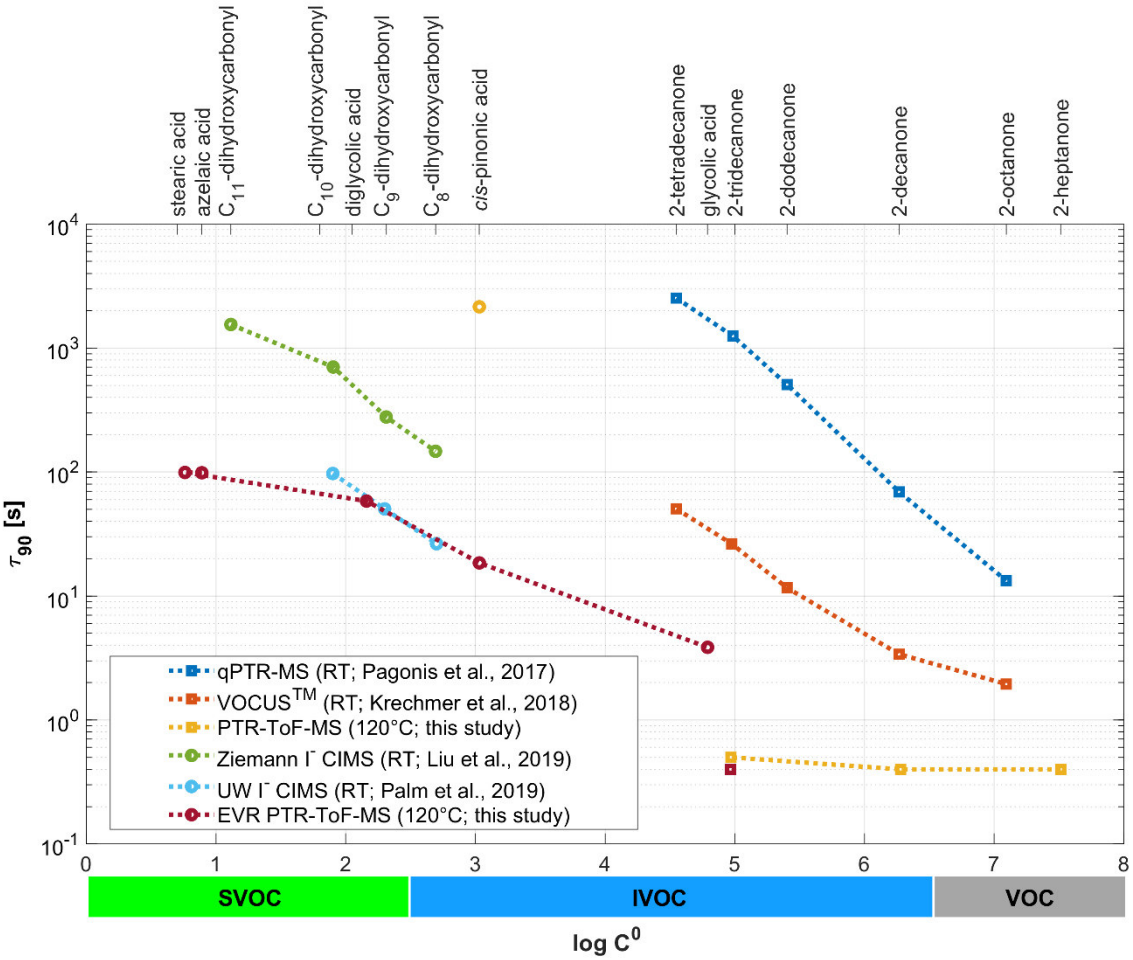

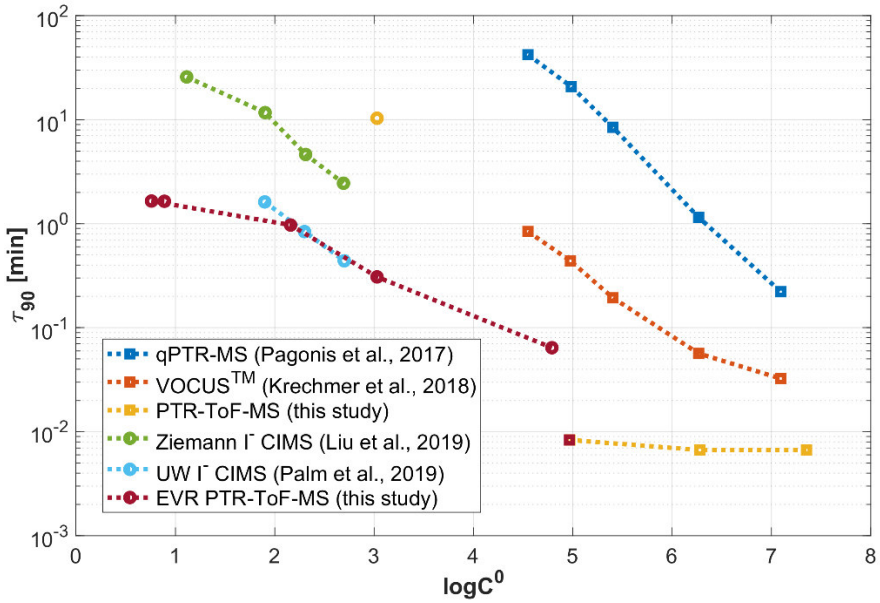

395

Figure 64. Signal decay times (here reported as τ_{90}) as observed in different online CIMS instruments for a set of ketones, carboxylic acids and dihydroxycarbonyls. τ_{90} is plotted as a function of the SIMPOL.1-derived saturation mass concentration ($\log C^0$).

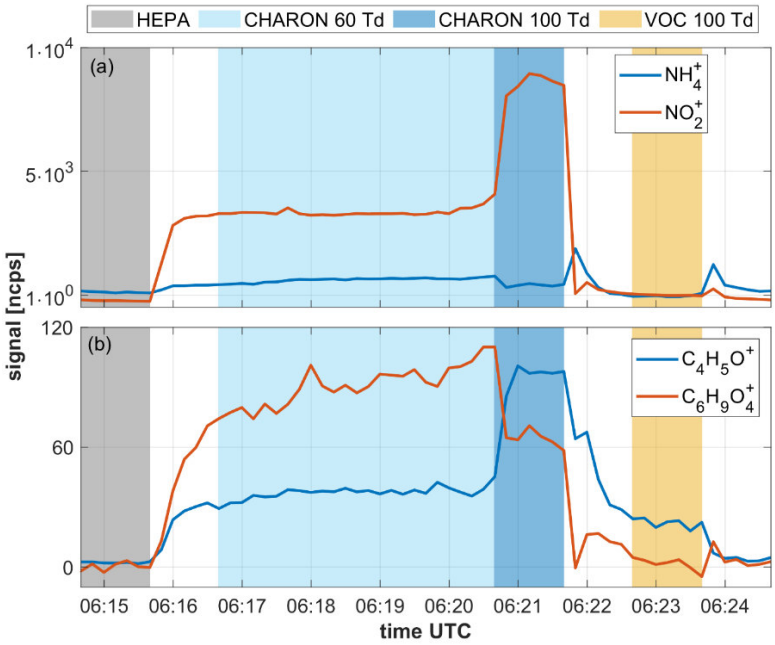

Figure 7~~5~~. Time series showing various analyte signals as recorded during a 10-minute measurement cycle of ambient air. The 10-min measurement cycle included: i) 1 min of instrumental background measurements with the CHARON inlet including a HEPA filter, ii) 4 mins of particulate measurements at an E/N of 60 Td, iii) 1 min of particulate measurements at an E/N of 100 Td and iv) 1 min of gas measurements at an E/N of 100 Td. The benefit of measuring particles at 60 and 100 Td is explained in Leglise et al. (2019) and is not discussed here. The CHARON inlet enriched the particle concentration by a factor of ~20, which explains the higher signal intensities in the particle measurement (in blue) as compared to the gas measurement (in yellow).

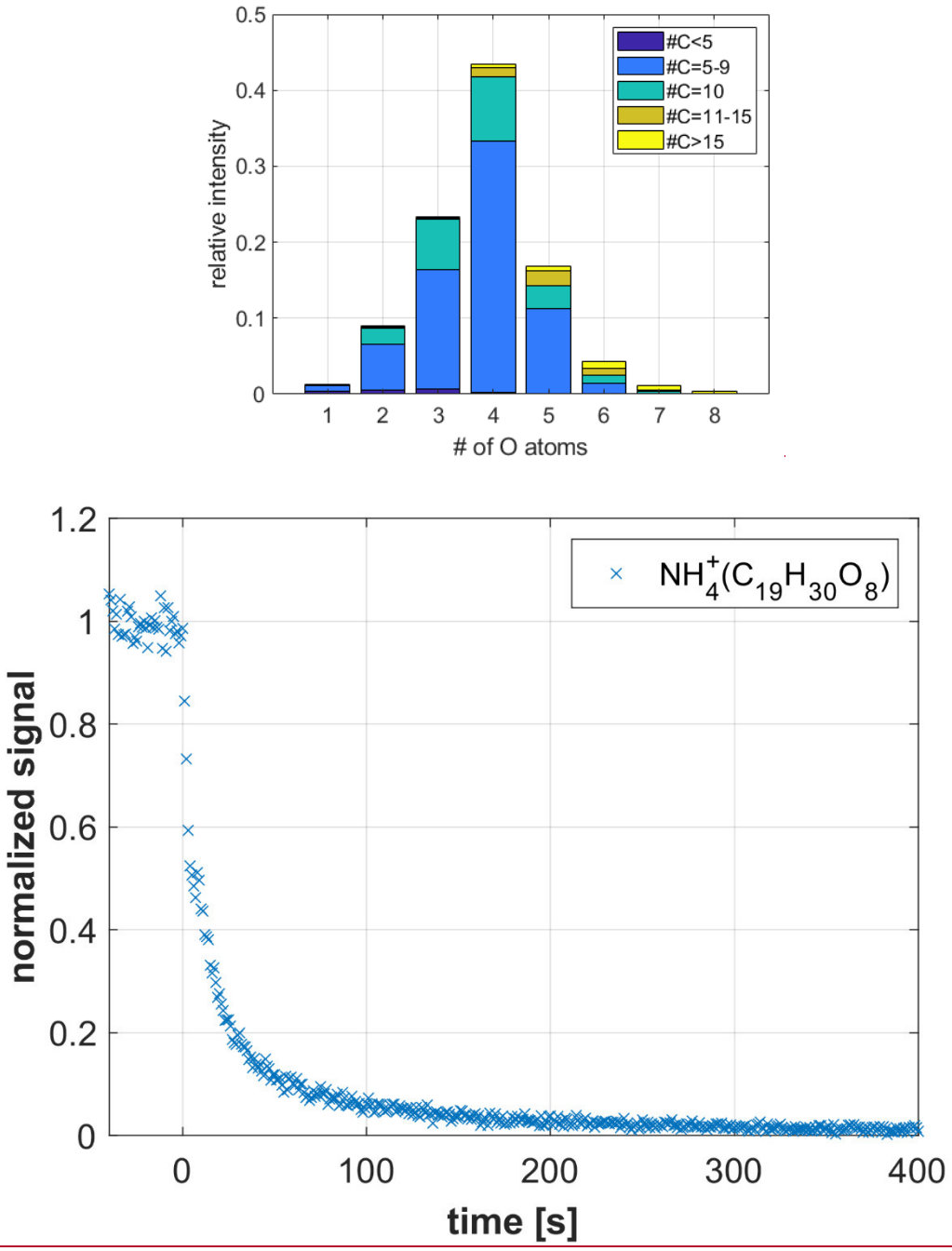

Figure 86: Decay of the $NH_4^+(C_{19}H_{30}O_8)$ signal as recorded by a CHARON EVR PTR-MS analyzer when O_3/limonene SOA was sampled and the instrument was switched from the CHARON particle inlet to the gas inlet at t=0.

~~Normalized mass distribution as a function of the number of oxygen atoms (#O) that was observed when the CHARON EVR PTR-MS analyzer sampled SOA generated from the reaction of limonene with ozone. The color code indicates the number of carbon atoms (#C). Mass concentrations were derived from the assumption that all analytes form ammonium adducts at the collisional rate (Zaytsev et al., 2019).~~